Korean J. Chem. Eng., **23**(4), 522-530 (2006)

Simulation of fixed bed reactor for dimethyl ether synthesis

Shin Beom Lee, Wonjun Cho*, Dal Keun Park and En Sup Yoon†

School of Chemical Engineering, Seoul National University, San 56-1 Sillim-dong, Gwanak-gu, Seoul 151-742, Korea
*LNG Technology Research Center, KOGAS, Dongchun-dong, Yeonsu-gu, Incheon 406-130, Korea
(*Received 8 June 2005 • accepted 7 March 2006*)

Abstract−Dimethyl Ether (DME) is considered as one of the most promising candidates for a substitute for LPG and diesel fuel. We analyzed one-step DME synthesis from syngas in a shell and tube type fixed bed reactor with consideration of the heat and mass transfer between catalyst pellet and reactants gas and effectiveness factor of catalysts together with reactor cooling through reactor wall. Simulation results showed strong effects of pore diffusion. We compared two different arrangements of catalysts, mixture of catalyst pellets (methanol synthesis catalyst and methanol dehydration catalyst) and hybrid catalyst. Hybrid catalyst gave better performance than a mixture of pellets in terms of CO conversion and DME productivity, but more difficulties with reactor temperature control. Use of inert pellets and inter-cooling was also simulated as a means of controlling maximum reactor temperature.

Key words: Reactor, Modelling, Dimethyl Ether, DME, Fixed Bed, Simulation, Effectiveness Factor

INTRODUCTION

Dimethyl ether (DME), the simplest ether, is a colorless, non-toxic, environmentally benign compound. It is currently used as a solvent and propellant in various aerosol products. Its physical properties closely resemble those of liquefied petroleum gas (LPG). DME is considered as a substitute for diesel fuel. Compared with diesel fuel combustion, DME produces much less pollutants such as carbon monoxide, nitrogen oxides and particulates. DME is traditionally produced by dehydration of methanol, which is in turn produced from syngas, products of natural gas reforming. This traditional process is thus called a two-step or indirect method of DME preparation. However, DME can be prepared directly from syngas (single-step or direct method). Single-step method needs only one reactor for DME synthesis, instead of two for two-step process. It can also alleviate thermodynamic limitation of methanol synthesis by converting it as produced into DME, thereby potentially enhancing overall conversion of syngas to DME. Catalysts are required for the conversion of syngas to DME. Control of reactor temperature is very critical as DME synthesis is strongly exothermic. Fluidized bed reactor is proposed as an ideal reactor for the highly exothermic DME synthesis [Lu et al., 2004]. But the study on fluidized bed reactors is in the initial stage of the laboratory scale, and its feasibility is not yet established. Investigators are studying two different reactor types for the commercialization of DME synthesis: bubbling slurry reactor and fixed bed reactor. In a slurry reactor fine catalyst particles are suspended in a solvent and feed gas enters as bubbles from below. Control of reactor temperature is manageable due to large heat capacity of the solvent that is cooled by heat exchange tubes in the reactor. But reactant should be transferred from gas bubbles to liquid phase solvent and then to catalyst particles for the synthesis reaction. Low diffusivity in the liquid phase can slow down overall reaction rate. Loss of fine catalyst particles from the reactor could also be a problem. Much empiricism would be needed for scale-up of the process. Fixed bed DME process can potentially solve those problems.

In a fixed bed reactor the main difficulty would be the prevention of the occurrence of hot spots. Catalysts can be irreversibly deactivated once exposed to above certain temperatures. One simple way of limiting temperature rise is controlling conversion, but this is not desirable economically. It is thus necessary to be able to understand and predict the reactor behaviour at various conditions for the design and scale-up of the DME synthesis process. But it is not practical to gather all the data experimentally, and numerical simulation will be very valuable in the process development. In this study we developed a mathematical model to simulate a pilot-plant scale, shell and tube type DME reactor. Syngas feed to the reactor is provided from reforming of re-evaporated LNG. We considered chemical reactions, heat transfer and mass transfer between the catalyst and bulk fluid, pore diffusion within the catalyst pellets, and heat transfer between the reactant stream in tubes and cooling medium in the shell. We considered two different cases for the catalyst. One involves using a mixture of methanol synthesis catalyst pellets and DME synthesis catalyst pellets (mixture of pellets). The other one is using hybrid catalyst pellet prepared from mixture of ingredients for methanol synthesis and those of DME synthesis (hybrid catalyst). We investigated the effects of various variables on the performance of the reactor.

REACTOR MODEL DEVELOPMENT

1. Reaction Kinetics

Preparation of DME from syngas can be represented by three catalytic reactions as shown below [Ng et al., 1999].

$$CO_2+3H_2 \leftrightarrow CH_3OH+H_2O \quad (1a)$$

$$CO+H_2O \leftrightarrow CO_2+H_2 \quad (1b)$$

$$2CH_3OH \leftrightarrow CH_3OCH_3+H_2O \quad (1c)$$

Reaction (1a) is a methanol synthesis reaction from carbon dioxide

†To whom correspondence should be addressed.
E-mail: esyoon@pslab.snu.ac.kr

and hydrogen. Reaction (1b) is a water gas shift reaction. These two reactions are catalyzed by methanol synthesis catalyst ($CuO/ZnO/Al_2O_3$). Reaction (1c) is methanol dehydration reaction: DME synthesis reaction catalyzed by an acidic catalyst (γ-alumina). Combinations of these three reactions can explain other schemes of DME preparation from syngas. And we use reaction rate equations as follows: [Busshe et al., 1996; Bercic et al., 1992].

$$r_{CO_2\ hydrogenation}=\frac{k_1(p_{H_2}p_{CO_2})[1-(1/K_{eqm1})(p_{CH_3OH}p_{H_2O})/(p_{CO_2}p_{H_2}^3)]}{(1+K_2(p_{H_2O}/p_{H_2})+\sqrt{K_3p_{H_2}}+K_4P_{H_2O})^3}$$

$$\Delta Hr=-49.47\ kJ/mol \tag{2a}$$

$$r_{RWGS}=\frac{k_5p_{CO_2}[1-K_{eqm2}(p_{CO}p_{H_2O}/p_{CO_2}p_{H_2})]}{1+K_2(p_{H_2O}/p_{H_2})+\sqrt{K_3p_{H_2}}+K_4P_{H_2O}}$$

$$\Delta Hr=41.17\ kJ/mol \tag{2b}$$

$$r_{MeOH\ dehydration}=k_6K_{CH_3OH}^2\left[\frac{C_{CH_3OH}^2-(C_{H_2O}C_{DME}/K_{eqm3})}{(1+2\sqrt{K_{CH_3OH}C_{CH_3OH}}+K_{H_2O}C_{H_2O})^4}\right]$$

$$\Delta Hr=-21.003\ kJ/mol \tag{2c}$$

These three reactions are all exothermic. The adiabatic temperature rise can be more than 1000K if the reactions could be sustained to completion. Therefore, handling of reaction heat is very important for the control of reactions. Values of kinetic parameters in the above kinetic expressions are summarized in Table 1.

$$Log_{10}K_{eqm1}=\frac{3066}{T}-10.592 \tag{3a}$$

$$Log_{10}\frac{1}{K_{eqm2}}=-\frac{2073}{T}+2.029 \tag{3b}$$

$$Log_{10}K_{eqm3}=\frac{10194}{T}-13.91 \tag{3c}$$

Equilibrium constant of each reaction is taken from literature [Twigg, 1986; Stull et al., 1969].

2. Heat and Mass Transfer on the Surface of the Catalyst

Due to the highly exothermic nature of the reactions, the temperature of the catalyst pellets can be different from bulk stream of the reactants. Likewise, there could be a difference in reactant concentration between the bulk and catalyst pellet surface. Therefore, we investigated heat and mass transfer on the surface of the catalyst pellets. We employed conventional expressions for the heat transfer coefficient: [Kunii et al., 1990; Welty et al., 1976; Cengel, 1998].

Table 1. kinetic parameters

	A(i)	B(i)	Parameter
k_1	1.65	36696	4846.93
K_2	3610	0	3610
K_3	0.37	17197	15.61
K_4	7.14×10^{-11}	124119	38.34
k_5	1.09×10^{10}	−94765	12.07
K_{ch3oh}	0.00079	70500	3633.13
k_6	3.7×10^{10}	−105000	4.417
K_{H2O}	0.084	41100	643.376

Parameter=A(i) exp(B(i)/RT)

$$N_{nu}=\frac{h_pd_p}{k_g}=2+0.6N_{Resph}^{0.5}N_{pr}^{1/3} \tag{4}$$

$$N_{Resph}=\frac{d_pv\rho}{\mu}$$

$$N_{pr}=\frac{C_p\mu}{k_g}$$

The temperature of the catalyst particles should satisfy an energy balance of heat transfer and heat of reaction. Because of steady state, reaction heat should be equal to the heat transferred between the surface of the catalyst and the reaction fluid.

$$\sum_i r_i\Delta H_r g_{cat}=h_pA_p(T_{p1}-T_f) \tag{5}$$

3. Effectiveness Factor

Intrinsic reaction rate can be different from global reaction rate because of pore diffusion in the catalyst pellet when the diameter of the catalyst pellet is several millimeters. We assume the temperature in the catalyst pellet is equal to the temperature in the surface of the catalyst pellet and only consider mass balance in it. For spherical catalyst pellets, if concentrations of reactants on catalyst surface are C_o, radius of a particle is R, concentration of reactants and products can be obtained by solving the following equations [Satterfield, 1970].

$$\frac{d^2C_{H_2}}{dr^2}+\frac{2}{r}\frac{dC_{H_2}}{dr}=\frac{3\rho_{p_1}}{D_{eff.H_2}}r_{CO_2}+\frac{\rho_{p_1}}{D_{eff.H_2}}r_{RWGS} \tag{6a}$$

$$\frac{d^2C_{CO}}{dr^2}+\frac{2}{r}\frac{dC_{CO}}{dr}=-\frac{\rho_{p_1}}{D_{eff.CO}}r_{RWGS} \tag{6b}$$

$$\frac{d^2C_{CO_2}}{dr^2}+\frac{2}{r}\frac{dC_{CO_2}}{dr}=\frac{\rho_{p_1}}{D_{eff.CO_2}}r_{CO_2}+\frac{\rho_{p_1}}{D_{eff.CO_2}}r_{RWGS} \tag{6c}$$

$$\frac{d^2C_{H_2O}}{dr^2}+\frac{2}{r}\frac{dC_{H_2O}}{dr}=-\frac{\rho_{p_1}}{D_{eff.H_2O}}r_{CO_2}-\frac{\rho_{p_1}}{D_{eff.H_2O}}r_{RWGS}-\frac{\rho_{p_2}}{2D_{eff.H_2O}}r_{MeOH} \tag{6d}$$

$$\frac{d^2C_{DME}}{dr^2}+\frac{2}{r}\frac{dC_{DME}}{dr}=-\frac{\rho_{p_2}}{2D_{eff.DME}}r_{MeOH} \tag{6e}$$

$$\frac{d^2C_{MeOH}}{dr^2}+\frac{2}{r}\frac{dC_{MeOH}}{dr}=-\frac{\rho_{p_1}}{D_{eff.MeOH}}r_{CO_2}+\frac{\rho_{p_2}}{D_{eff.MeOH}}r_{MeOH} \tag{6f}$$

Boundary Conditions

$$r=R,\ C=C_o$$

$$r=0,\ \frac{dC}{dr}=0$$

Effective diffusivity of gases through porous catalyst pellets was estimated from molecular diffusivity, porosity and tortuosity of pores:

$$D_{eff.i}=D_i\frac{\varepsilon}{\tau} \tag{7}$$

ε=void fraction (porosity)
τ=tortuosity

We employed 0.603 for porosity and 3 for tortuosity, respectively [Bercic et al., 1992]. Solutions of these equations provide the concentration profiles of gas species in the catalyst pellets together with the global reaction rates.

4. Heat Transfer between Tubes and Shell

Heat generated from the chemical reactions in the catalyst is transferred to the gases flowing through reactor tubes, and then to cooling

medium in the shell side of the reactor. The overall heat balance can be summarized as follows:

$$(\sum_i r_i \Delta H_r g_{cat} - U A_t (T_f - T_o)) = C_{p,fluid} m_f \Delta T_f \quad (8)$$

Eq. (8) holds for the whole reactor as well as any section of it. It calculates temperature rise of the reactants by subtracting heat transfer to coolant from heat generated by chemical reactions. In order to estimate the heat transfer coefficient, U, we should know both shell side and tube side heat transfer coefficients. The common method of heat transfer coefficient calculation procedures can be employed for the estimation of shell side heat transfer coefficient as heat transferring liquid or boiling water is used as cooling medium in the shell [McCabe et al., 1995].

$$U_o = \frac{1}{\frac{1}{h_i}\left(\frac{D_o}{D_i}\right) + \frac{x_w}{k_m}\left(\frac{D_o}{D_L}\right) + \frac{1}{h_o} + \frac{D_o}{D_i}\frac{1}{h_{di}} + \frac{1}{h_{do}}} \quad (9a)$$

$$h_o = \frac{0.023 C_p v \rho}{N_{pr}^{2/3} N_{re}^{0.2}} \quad (9b)$$

But the presence of catalyst pellets makes the estimation of heat transfer coefficient on the tube side quite complicated. Although several correlations are available in the literature, their reliability should be experimentally verified. As we do not have experimental values for the tube side heat transfer coefficient, we selected the following correlation for the estimation of tube side heat transfer coefficient [Kunii et al., 1990].

$$h = \left(\frac{1}{\frac{1}{h_r + 2k_{ew}^0/d_p + a_w C_{pg} \rho_g v} + \frac{1}{h_{packet}}} \right) \quad (10)$$

$$h_{packet} = 1.13 \left(\frac{k_e^0 \rho_p (1-\varepsilon_{mf}) C_{ps}}{\tau_i} \right)^{0.5}$$

$$k_{ew}^0 = \varepsilon_w k_g + (1-\varepsilon_w) k_s \left(\frac{1}{\phi_w (k_s/k_g) + 1/3} \right)$$

$$k_e^0 = \varepsilon_{mf} k_g + (1-\varepsilon_{mf}) k_s \left(\frac{1}{\phi_b (k_s/k_g) + 2/3} \right)$$

a_w=0.05, h_r (radiation)=0

5. Simulation of the Reactor

The next equation is used for mass flowrate profile in the tube of the reactor [Riggs, 1994].

$$\frac{dF_i}{dz} = \rho_b \frac{\pi D_t^2}{4} \sum_{j=1}^{n_r} \gamma_{i,j} r_j \quad i=1, 2, \ldots, n_c \quad (11)$$

For solving ODE, axial length of the reactor tube is divided into 1000 sections. First, reaction rates are calculated with the use of correlations listed in section 2.1. For this calculation heat and mass transfer on the surface of the catalyst of section 2.3 and effectiveness factor of section 2.3 are incorporated in order to reflect the effects of them on the reaction rates. Then correlations of section 2.4 are used for the calculation of reactor temperature in each section. Iterative procedures for determining temperature and reaction rates in each section are necessary as temperature and reaction rates are interdependent. After the temperature in the section of the tube is determined, a mass balance is calculated by using Eq. (11) in each section and then going to the next step. For the simulation of the fixed bed reactor, visual C++/visual FORTRAN programming tools were used and the whole procedure flowchart is depicted in Fig. 1.

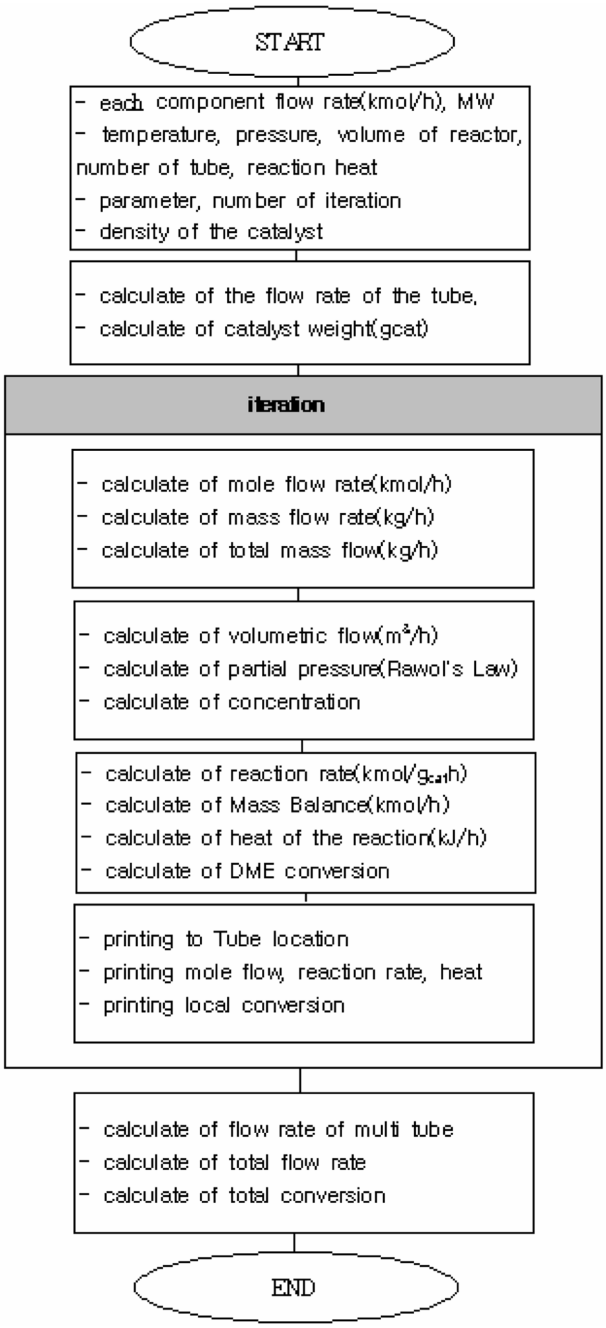

Fig. 1. Flowsheet of main module for the fixed bed reactor simulation.

This program can simulate the performance of the fixed bed reactor taking account of chemical reaction kinetics, heat and mass transfer between catalyst pellets and bulk fluid, effects of mass transfer inside each catalyst (effectiveness factor), heat transfer between fluids in the tubes and cooling medium in the shell. It can also calculate change of chemical species concentration as reactants gas stream move downward through reactor tubes filled with catalyst

pellets. Radial variation across tube diameter was neglected, as ratio of tube diameter to length is small.

We used the following correlations to evaluate reactor performance such as CO conversion, DME Yield, DME productivity:

$$\text{COconversion} = \frac{\text{COin} - \text{COout}}{\text{COin}} \times 100 \quad (12a)$$

$$\text{DMEyield} = \frac{\text{DMEout} \times 2}{\text{COin} - \text{COout}} \times 100 \quad (12b)$$

$$\text{DMEproductivity} = \frac{\text{DMEout}}{\text{mass of catalyst}} \quad (12c)$$

RESULTS AND DISCUSSION

Using the simulator we developed, we studied the behavior of a pilot-scale DME reactor. Reaction condition of the reactor for simulation is as follows: GHSV 1,000 hr^{-1}, feed temperature 280 °C, reactor pressure 50 bar, H_2 : CO ratio 2 : 1.

1. Effectiveness Factor of the Catalyst Pellet

The simulator evaluates effectiveness factor of the catalyst pellets by solving mass balance equations for pore diffusion and chemical reactions within the catalyst pellet. Fig. 2 and Fig. 3 show profiles of reaction rates within catalyst pellets for the case of mixture of pellets. In this case catalyst pellets for the synthesis of methanol from syngas ($CuO/ZnO/Al_2O_3$, 6 mm pellets for reaction 1 and 2) and catalyst pellets for the synthesis of DME by dehydration of methanol (γ-alumina, 7.7 mm pellets for reaction 3) are present as a mixture inside the reactor tubes. We can observe strong influence of pore diffusion on reaction rate. Reaction rate of water gas shift decreased in the catalyst core by pore diffusion effect of CO. But, reaction rates of methanol synthesis showed a maximum value in the region about 2.5-3 mm from the catalyst surface. It was caused by CO_2 increase from water gas shift reaction.

Note that methanol dehydration occurs only on the methanol dehydration catalyst in the case of mixture of pellets. Thus, Fig. 3 shows effects of pore diffusion on reaction rate. However, quite a different picture emerges in the case of hybrid catalyst (Fig. 4). Here all three reactions occur in the same catalyst pellet. Although reaction rate of water gas shift reaction decreases toward the center of the catalyst pellet as a result of pore diffusion effects, reaction rates of methanol synthesis and DME synthesis in the core region of the catalyst pellets are higher than those of near pellet surface. As the reactions (1), (2) and (3) involved in the synthesis of methanol and DME are interrelated in a complex way including pore diffusion, their rates within the catalyst pellet reflect inter-play of mass transfer and chemical reactions as well as variations of species concentra-

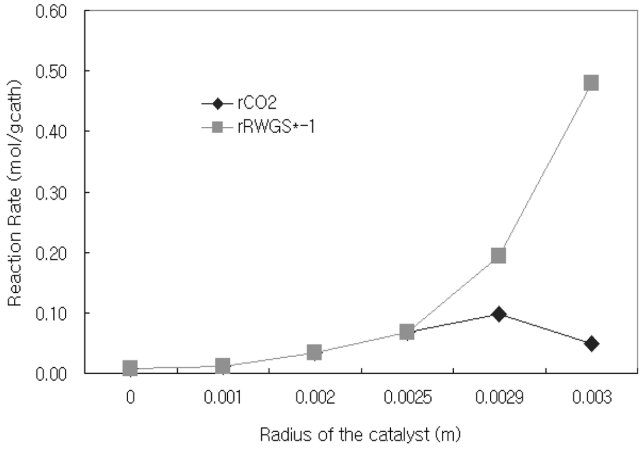

Fig. 2. Reaction rate of CO_2 hydrogenation and water gas shift in methanol synthesis catalyst.

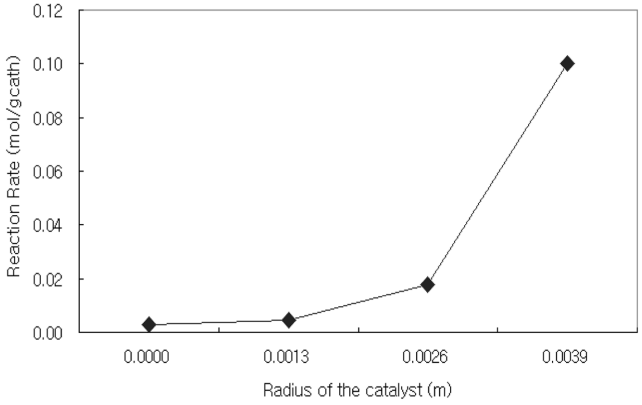

Fig. 3. Reaction rate of methanol dehydration in methanol dehydration catalyst.

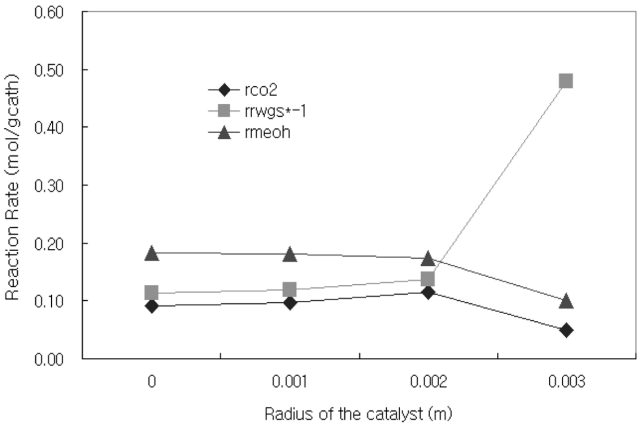

Fig. 4. Reaction rate of CO_2 hydrogenation, water gas shift and methanol dehydration in hybrid catalyst.

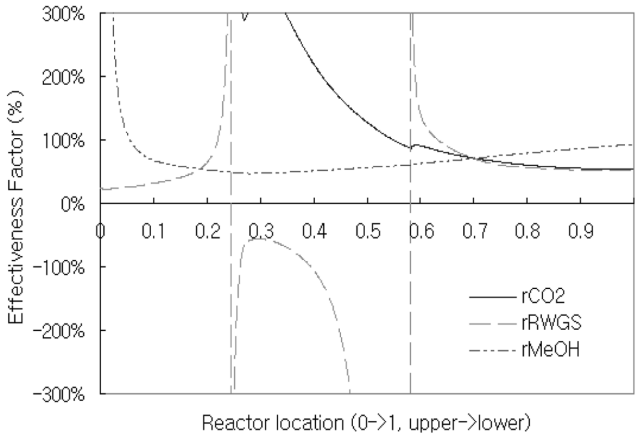

Fig. 5. Effectiveness factor vs. Reactor location.

tion within the catalyst. Therefore, the effectiveness factor can be over 100% under some circumstances for hybrid catalysts. We evaluated the effectiveness factor for three reactions along the reactor length and found that effectiveness factor for DME synthesis reaction is well over 100% in the entrance zone of the reactor, and that for methanol synthesis above 100% in the first half of the reactor (Fig. 5). The effectiveness factor for the water shift reaction shows a very unusual trend. It swings from negative and positive values. In order to investigate this further, we calculated effectiveness factors for various sizes of catalyst pellets.

Fig. 5 shows that effectiveness factors approach to 1 with decrease of catalyst size as expected. There are no negative values for effectiveness factor in this figure. But Fig. 7 shows that for catalyst pellets beyond a certain size, 0.4-0.5 mm in this case, the effectiveness factor for the water shift reaction is negative. The difference between Fig. 6 and Fig. 7 is that the former is for the reaction conditions near reactor entrance and the latter for the reactor mid-section, that is, difference in species concentration (See Fig. 5). Am effectiveness factor can have negative values when reaction condition allows a reversible reaction to proceed.

2. Reactor Performance in the Case of Mixture of Pellets

Fig. 8 shows reactor behavior for the case of a mixture of pellets. It shows the temperature of reactant stream rises rapidly (280 to 321 °C) and then falls slowly as it moves down through reactor tube. It means cooling is not sufficient in the entrance region of the reactor

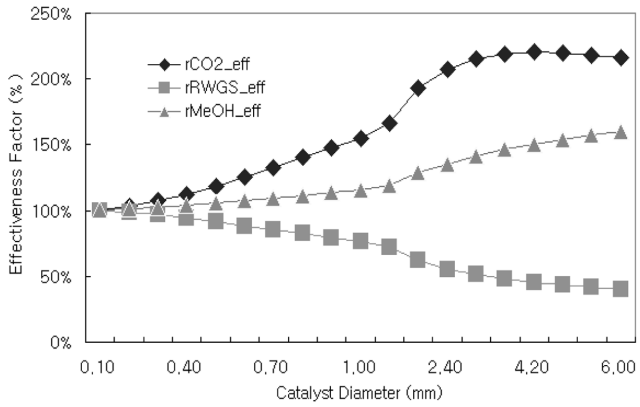

Fig. 6. Effectiveness factor versus catalyst diameter near the reactor entrance.

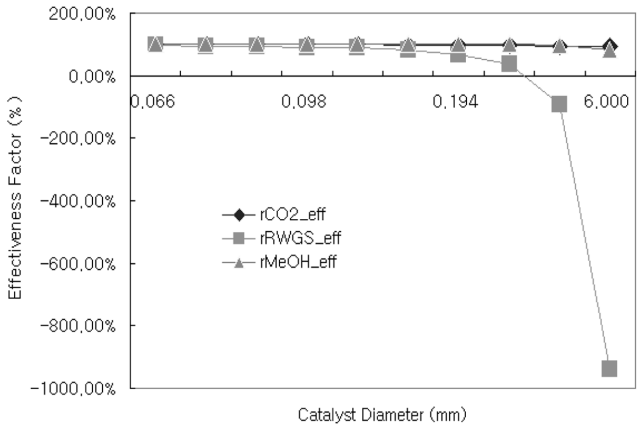

Fig. 7. Effectiveness factor versus catalyst diameter at the middle section of the reactor.

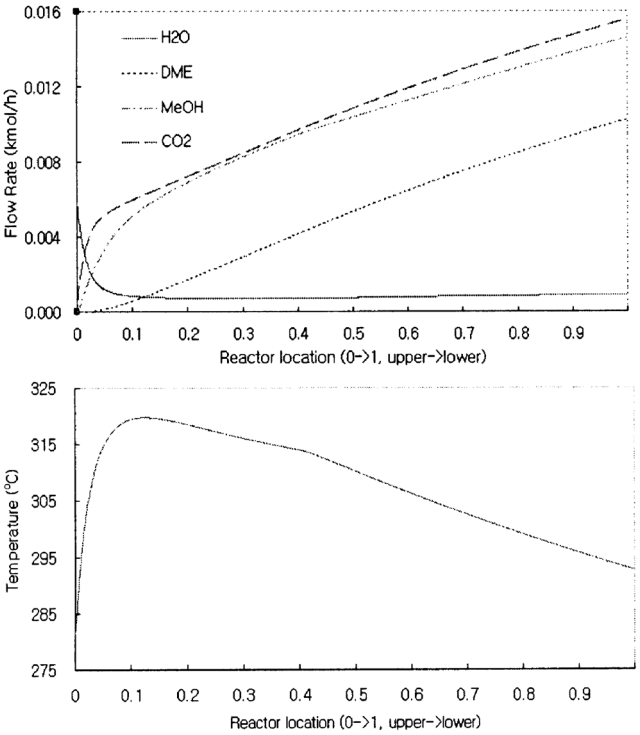

Fig. 8. Flow rate and temperature profile in the fixed bed reactor for DME synthesis (in the case of mixture of pellets: 80% methanol synthesis catalyst, 20% methanol dehydration catalyst).

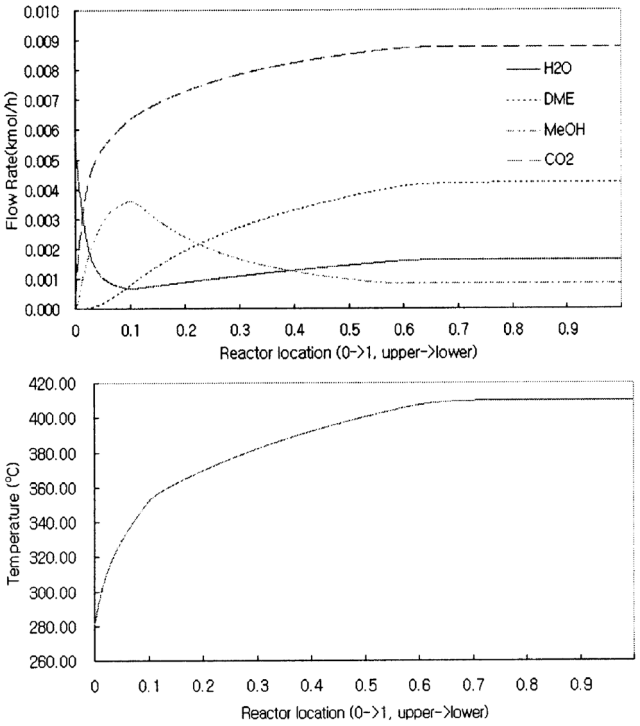

Fig. 9. Flow rate and temperature profile of the reactor operated adiabatically (all the other conditions are the same as Fig. 8).

where chemical reactions are fast due to high concentration of reactants. In the case of mixture of catalyst pellets CO conversion is 40.2% and DME productivity is 9.4 gmol/kg-cat h.

As we notice in Fig. 8, maintaining uniform temperature along the reactor length is not a trivial problem due to the highly exothermic nature of the reactions involved in DME synthesis even with shell and tube type reactor design. When no cooling is used, i.e., in the case of adiabatic operation, temperature will rise along the reactor length all the way to the reactor exit (Fig. 9). Maximum temperature in this case is 409.8 °C. At this high temperature water gas shift reaction is accelerated;, thus CO_2 concentration is high and methanol, DME are very low because of decreasing of CO_2 hydrogenation and methanol dehydration. However, catalyst deactivation could be very serious at high temperatures, so operation above a certain, catalyst specific, temperature should be avoided. In the case of adiabatic operation in the absence of catalyst deactivation problem, CO conversion is 14.2% and DME productivity is 3.86 gmol/kg-cat h.

We studied effects on the reactor performance of operation variables such as feed temperature, GHSV (Gas Hourly Space Velocity), H_2 : CO ratio in the feed gas, reactor pressure and ratio of methanol synthesis catalyst to methanol dehydration catalyst. Fig. 10(a) shows that within the feed temperature range of 200-350 °C, the higher the feed temperature, the better DME productivity could be

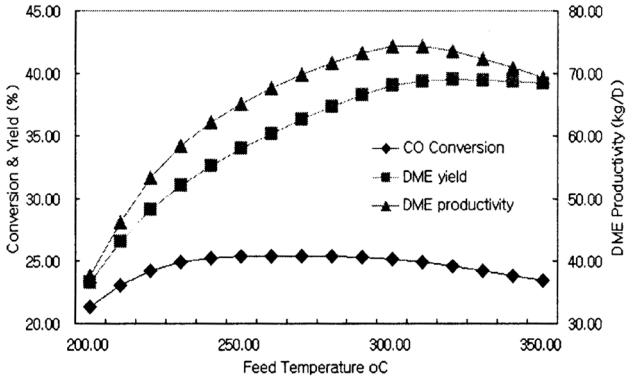

(a) Effects of feed temperature on the reactor performance

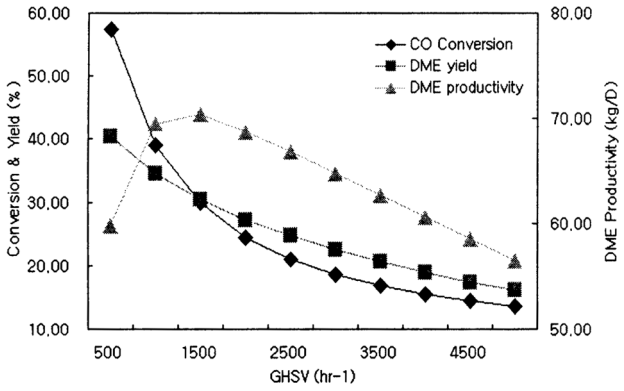

(b) Effects of GHSV on the reactor performance

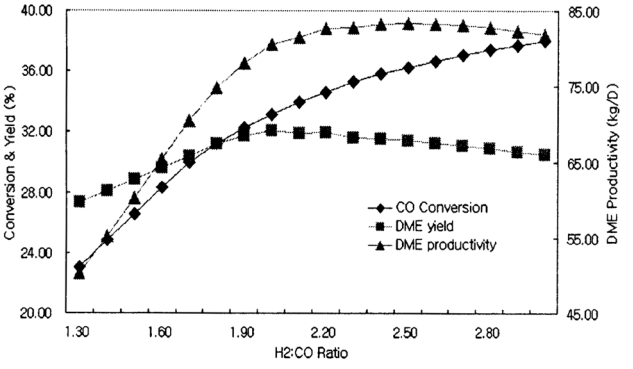

(c) Effects of H_2:CO ratio in the feed gas on the reactor performance

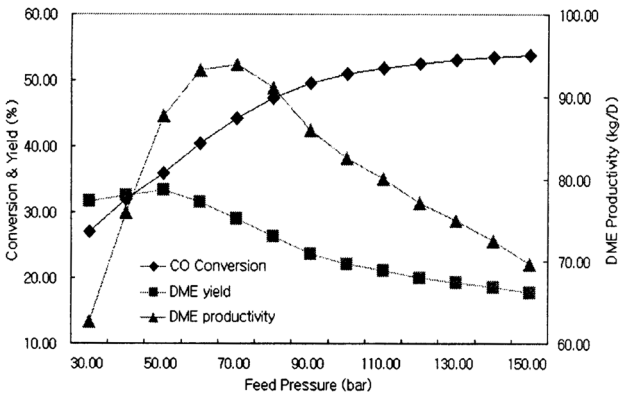

(d) Effects of reactor pressure on the reactor performance

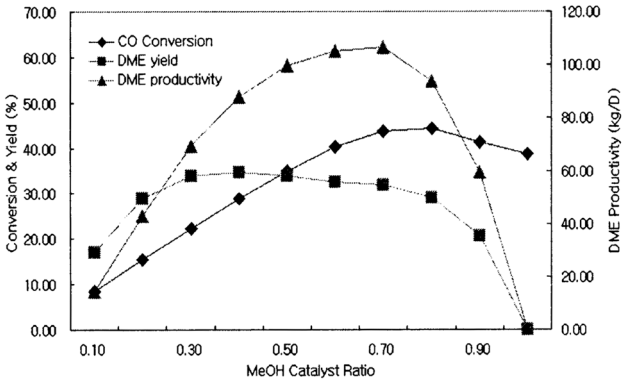

(e) Effects of methanol synthesis catalyst to methanol dehydration catalyst ratio on the reactor performance

Fig. 10. Effects of operation parameters on the reactor performance in the case of mixture of pellets.

obtained. But there is an optimum temperature for the maximum CO conversion. So DME productivity is highest at a feed temperature of 300 °C.

At low values of GHSV, residence time in the reactor is large, so CO conversion and DME yield are high. But feed rate is small with low GHSV, and productivity can be small as well (See Fig. 10(b)). On the other hand, at high value of GHSV residence time is small, so conversion and yield are low. Therefore, there is an optimum value of GHSV for the maximum DME productivity. Fig. 10(b) shows DME productivity is largest when GHSV is 1,500 within the GHSV range of 500-5,000.

The ratio of H_2 : CO in syngas varies depending on the feed stock to reforming and post-treatment of syngas. We studied the effects of H_2 : CO ratio in the feed gas on the reactor performance by varying its value within the range 1.3-3.0. When the ratio is low, CO_2 hydrogenation decreased. This causes not enough water production for water gas shift reaction, thereby decreasing reaction rate of the latter. CO conversion increases with the H_2 : CO ratio. But due to excess water, methanol dehydration decreases at higher H_2 : CO ratio. The overall result is that DME productivity is about the same for the H_2:CO ratio of 1.8-2.8 (Fig. 10(c)).

Fig. 10(d) shows the effects of reactor pressure. As gas volume decreases with the synthesis of DME from syngas, higher pressure favor the reaction. Therefore, DME synthesis is practised at high pressures. Within the range 30-150 bar DME productivity was best at 70 bar.

The effects of the ratio of methanol synthesis catalyst to methanol dehydration catalyst are shown in Fig. 10(e). Note that the mixture of two different catalyst pellets is used and the ratio can be varied at will. With too little methanol synthesis, catalyst methanol synthesis catalyst DME production capability (i.e., methanol dehydration) cannot be fully utilized due to limited supply of methanol. On the other hand, the reaction rate of methanol dehydration will not be sufficient to process methanol in the case of too little dehydration catalyst in the reactor. In the extreme case of the ratio one or zero no production of DME will result. Fig. 10(e) shows that DME productivity is best when the reactor filled with 70% methanol synthesis catalyst and 30% methanol dehydration catalyst.

3. Reactor Performance in the Case of Hybrid Catalyst

Reactor performance for hybrid catalyst is shown in Fig. 11. In this case, hybrid catalyst consists of methanol synthesis component and methanol dehydration component whose ratio is 8 : 2. Maximum temperature in the reactor is 345 °C, higher than that of mixture of catalyst pellets, 320 °C (Fig. 8). In this case, CO conversion is 69.2%, DME productivity is 28.4 gmol/kg-cat h, higher than that of mixture of pellets. In hybrid catalyst active sites for methanol synthesis and methanol dehydration coexist, thereby realizing synergy effects of their proximity. In the case of a mixture of pellets it seems that the distance between catalysts is too large to realize synergy effects.

Fig. 12 shows the effects of composition of hybrid catalyst on the reactor performance. Comparing this with Fig. 10, we can notice that hybrid catalyst is much better than a mixture of pellets with regards to the reactor performance. Optimum ratio of catalyst components in this case is 50 : 50, compared to 70 : 30 in the case of mixture of pellets. Fig. 13 shows reactor performance for hybrid catalyst in the case of components ratio 50 : 50. Compared to components ratio 80 : 20, DME productivity is higher, but maximum temperature in the reactor is also higher (353 °C versus 345 °C).

As was observed in the above, higher maximum reactor temperature is an indication of better performance of the reactor. But it also means higher probability of experiencing hot spots. At high reactor temperature catalyst can deactivate irreversibly. In principle, reactor temperature can be controlled by rapid removal of reaction heat through high heat transfer coefficient (U), large heat exchange area (A_t) and temperature difference ($T_f - T_o$) (see Eq. (4)). Heat transfer coefficient is largely determined by the physical properties involved and operating conditions of the reactor. Large heat exchange area is rendered through employing smaller tubes with the result of in-

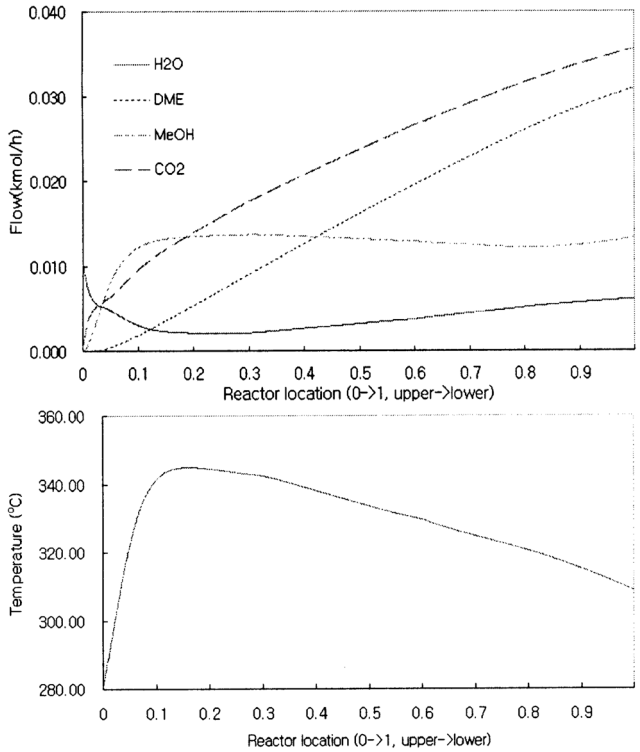

Fig. 11. Flow rate and temperature profile of the reactor filled by hybrid catalyst (methanol synthesis catalyst component 80%).

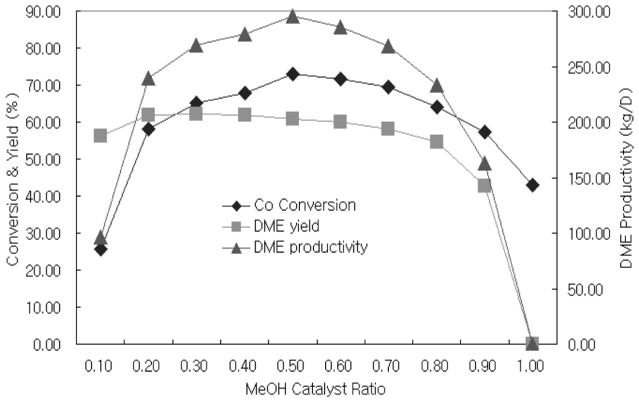

Fig. 12. Effects of catalyst components in hybrid catalyst.

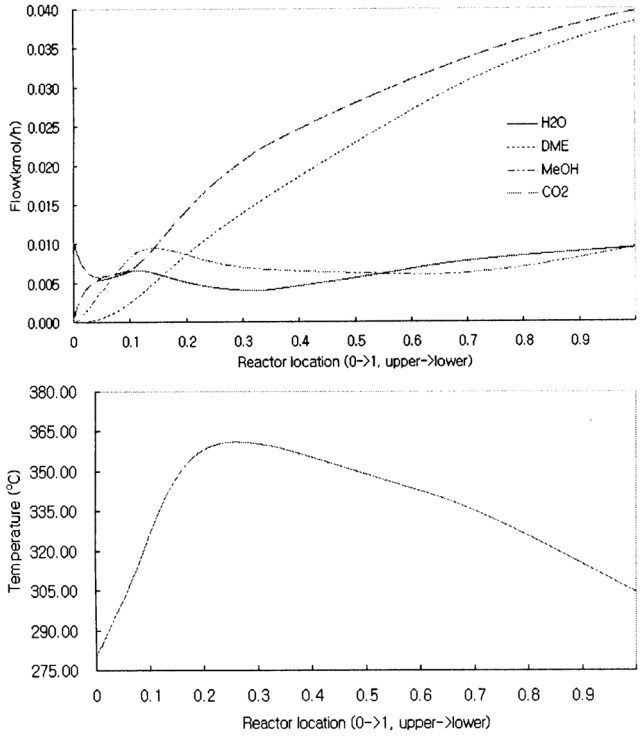

Fig. 13. Flow rate and temperature profile of the reactor filled with hybrid catalyst (methanol synthesis catalyst component ration 50%).

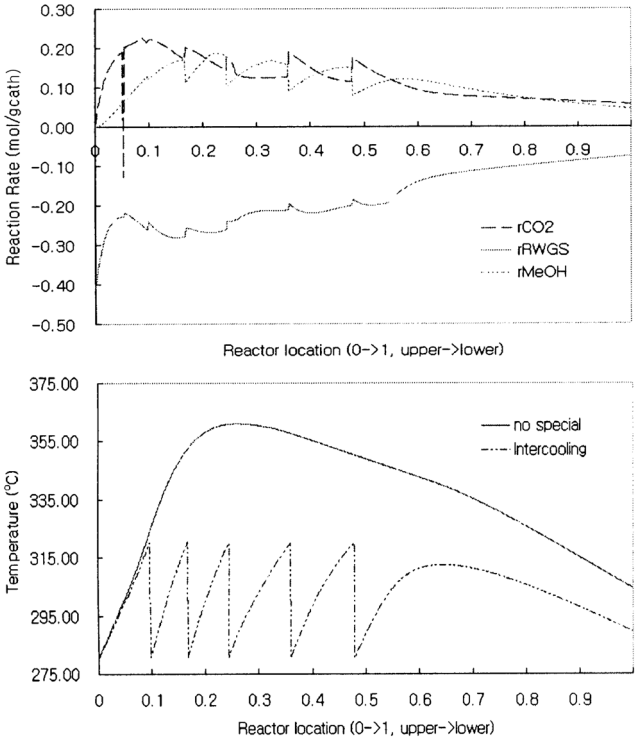

Fig. 15. Reaction rate and temperature profile with the intercooling.

crease in the number of tubes. There is also a limit to the size of tube that can accommodate catalyst pellets of a certain size. By the use of lower temperature for the cooling medium we can increase ($T_f - T_o$), But control and start-up of the reactor will impose a limit on feasible coolant temperature. Therefore, it is worthwhile to probe means to control maximum reactor temperature. We investigated two different schemes of shaving off maximum reactor temperature. One is filling a specified amount of inert catalyst pellets in the specific region of the reactor, and the other is inter-cooling of the reactor. In both cases the target is keeping the maximum reactor temperature below 320 °C. Fig. 14 shows a result of filling inert pellets in the reactor. In this case the region indicated in Fig. 14 (0.1-0.5 normalized reactor location) is filled with catalyst pellets 70%, inert pellets 30%. As the region (0.1-0.5 normalized reactor location) has less catalyst, reaction rate is slowed down with less release of reaction heat and less increase of temperature. In this case, temperature is controlled below 320 °C, but DME productivity is 29.26 gmol/kg-cat h, 17% less than normal case.

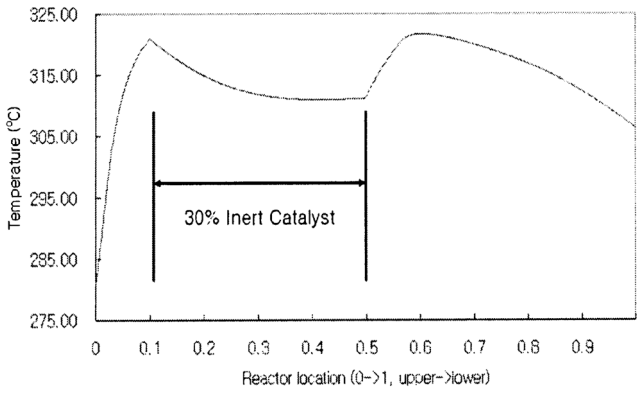

Fig. 14. Temperature profile of the reactor filled with 30% inert catalyst at 0.1-0.5 region.

Fig. 15 shows a reactor temperature profile in the case five-stage inter-cooling is applied in the first half of the reactor. Reactor temperature is controlled below 320 °C and DME productivity is 35.02 gmol/kg-cat h, similar with that of no special cooling method. But, inter-cooling needs additional equipment and is not flexible when the operation condition varies.

CONCLUSION

We developed a simulator of a shell and tube type fixed bed reactor for single-step DME synthesis from syngas. We examined behavior of the reactor at various conditions for the case of a mixture of pellets and hybrid catalyst. We found that complex reactions coupled with pore diffusion within the catalyst pellet affects can show unusual values of effectiveness factor. Employing hybrid catalyst yielded higher productivity compared with using a mixture of catalyst pellets. But, more careful cooling of reactor is needed as more reaction heat is released near the reactor entrance. For this, the method filling inert catalyst in the reactor and inter-cooling can be considered as a means of limiting maximum reactor temperature.

ACKNOWLEDGMENTS

Support of KOGAS and BK21 for this study is gratefully acknowledged.

NOMENCLATURE

A_t : surface area of the tube outside [m^2]
$C_{A0,i}$: concentration of component i in fluid [kmol/m^3]
D_{AB} : binary diffusivity [cm^2/s]
$D_{eff,i}$: binary effective diffusivity of component i in the catalyst pellet [m^2/h]
dHr, ΔHr : reaction Heat [kJ/mol]
g_{cat1} : mass of a MeOH synthesis catalyst [g]
g_{cat2} : mass of a MeOH dehydration catalyst [g]
K_i : adsorption constants
$K_{eqm,j}$: equilibrium constant of reaction j
m_f : mole flow rate of the fluid in a tube [g-mol/h]
n_c : number of components
n_r : number of reactions
r : particle radius [m]
r_{CO_2} : reaction rate of the methanol synthesis reaction [mol/gcat·h]
r_{RWGS} : reaction rate of the reverse water gas shift reaction [mol/gcat·h]
r_{MeOH} : reaction rate of the methanol dehydration (DME synthesis) reaction [mol/gcat·h]
T_f : fluid temperature [K]
T_o : coolant temperature [K]
T_{p1} : temperature of the MeOH synthesis catalyst [K]
T_{p2} : temperature of the MeOH dehydration catalyst [K]
U : overall heat transfer coefficient [J/m^2·h·°C]
$\gamma_{i,j}$: stoichiometry number of i-th component in j-th reaction
ρ_b : bed density of the catalyst

REFERENCES

Bercic, G. and Levec, J., "Intrinsic and global reaction rate of methanol dehydration over γ-Al_2O_3 pellets," *Ind. Eng. Chem. Res.*, **31**, 1035 (1992).
Cengel, *Heat transfer a practical approach*, McGrawHill (1998).
Kunii, D. and Levenspiel, O., *Fluidization engineering*, 2nd, Wiley (1990).
Lu, W.-Z., Teng, L.-H. and Xiao, W.-D., "Simulation and experiment study of dimethyl ether synthesis from syngas in a fluidized-bed reactor," *Chemical Engineering Science*, **59**, 5455 (2004).
McCabe, W. L., Smith, J. C. and Harriott, P., *Unit operations of chemical engineering*, 5th, McGrawHill (1995).
Ng, K. L., Chadwick, D. and Toseland, B. A., "Kinetics and modelling of dimethyl ether synthesis from synthesis gas," *Chemical Engineering Scienc*e, **54**, 3587 (1999).
Riggs, J. M., *An introduction to numerical methods for chemical engineers*, Texas Tech University Press (1994).
Satterfield, C. N., *Mass transfer in heterogeneous catalysis*, M.I.T. Press (1970).
Stull, D. R., Westrum, E. F. Jr. and Sinke, G. C., *The chemical thermodynamics of organic compounds*, John Wiley & Sons Inc. (1969).
Twigg, M. V., *Catalyst handbook*, 2nd, Wolfe (1986).
Vanden Busshe, K. M. and Froment, G. F., "A steady-state kinetic model for methanol synthesis and the water gas shift reaction on a commercial Cu/ZnO/Al_2O_3 catalyst," *Journal of Catalyst*, **161**, 1 (1996).
Welty, J. R., Wicks, C. E. and Wilson, R. E., *Fundamentals of momentum, heat and mass transfer*, 3rd, Wiley (1976).